PALAIOS
Emphasizing the impact of life on Earth's history

PALAIOS, 2011, v. 26, p. 545–554
Research Article
DOI: 10.2110/palo.2010.p10-133r

RECONSTRUCTING PALEOCATCHMENTS BY INTEGRATING STABLE ISOTOPE RECORDS, SEDIMENTOLOGY, AND TAPHONOMY: A LATE CRETACEOUS CASE STUDY (MONTANA, UNITED STATES)

BRADY Z. FOREMAN,[1]* HENRY C. FRICKE,[2] KYGER C. LOHMANN,[1] and RAYMOND R. ROGERS[3]
[1]University of Michigan, Department of Geological Sciences, Ann Arbor, Michigan 48109, USA, bradyf@umich.edu, kacey@umich.edu;
[2]Colorado College, Department of Geology, Colorado Springs, Colorado 80903, USA, hfricke@coloradocollege.edu; [3]Macalester College, Department of Geology, St. Paul, Minnesota 55105, USA, rogers@Macalester.edu

ABSTRACT

Robust isotopic reconstructions of climate, elevation, and biology require a reasonable capture of the range of isotopic variability across a paleolandscape. Here, we illustrate how integrating multiple proxies derived from a variety of paleoenvironments aids in this effort. We determined $\delta^{18}O$ and $\delta^{13}C$ values from lake and soil carbonates, unionid shells, gar scales, and crocodile teeth from multiple depositional environments (lakes, soils, ponds, streams, and large rivers) spanning a 300 km proximal-to-distal transect within the Late Cretaceous foreland basin of Montana. Two major patterns emerge. First, quiet water environments display higher $\delta^{18}O$ and lower $\delta^{13}C$ values than large rivers, which indicates greater input from local precipitation compared to high-altitude runoff, and a relatively larger contribution of degraded vegetative matter to the dissolved inorganic carbon load. Second, proxies with seasonal biases toward late spring and summer growth display lower $\delta^{18}O$ and $\delta^{13}C$ values in the basin proximal setting compared to the distal coastal setting, which is linked to the rainout history of vapor masses moving across the foreland basin. Overall these isotopic patterns mirror those in modern catchments, support hypotheses of monsoonal rainfall within the basin, and suggest a hypsometric mean elevation of ~2.6 km within the Sevier orogenic belt. Furthermore, our results indicate a potential to subdivide freshwater paleoecosystems to refine paleobiologic studies of habitat preference and migration patterns.

INTRODUCTION

Stable isotope records have proven an invaluable tool in paleoclimatic, paleogeographic, and paleobiologic reconstructions. Central to their application in the geologic record is understanding their systematic variation across modern landscapes. Initially, research focused on broad regional-to-global patterns in isotope compositions, for example the systematic decrease in $\delta^{18}O$ values of meteoric precipitation with increasing latitude, elevation, and distance traveled into continental interiors (Dansgaard, 1964; Rozanski et al., 1993; Gat, 1996). This research has become increasing geographically detailed and refined, spawning the field of isoscapes (West et al., 2010). Proxy-derived isotopic data from the geologic record, however, are comparatively coarse in their spatial and temporal resolution, due to (1) proxies record surface waters instead of direct meteoric precipitation; (2) seasonal preferences in biologic or authigenic growth and biologic behavior patterns; (3) the unevenness in the preservation proxy material (i.e., fossils) in the rock record; and (4) the geographic limits on outcrop exposure. Here, we illustrate how to overcome some of these issues by directly integrating multiple proxies with sedimentology, alluvial architecture, and taphonomy. Though the use of multiple isotopic substrates is not necessarily novel (e.g., Mulch and Chamberlain, 2007; Clementz et al., 2009; Amiot et al., 2010), the direct integration of substrates with detailed descriptions of depositional environments and taphonomic history is more rare (but see Morgan et al., 2009).

Here, we explore the benefits of this approach using the Campanian foreland basin of Montana as a case study. We compare $\delta^{18}O$ and $\delta^{13}C$ values from freshwater unionid bivalve shells (superfamily Unionacea), gar scales (family Lepisosteidae), crocodile teeth (order Crocodilia), pedogenic carbonate nodules, and lacustrine carbonates derived from a diverse suite of lithofacies representing large trunk or main stem rivers, tributary streams, ponds, large lakes, and soils. The sample sites are constrained to 75 ± 1 Ma based on dated bentonite horizons (Rogers et al., 1993; Foreman et al., 2008), and thus represent a snapshot of paleohydrologic conditions across ~300 km in the basin. This multi-proxy, multi–depositional environment approach creates an isotopic framework that incorporates records with varying biologic behaviors (mobile vs. sessile, aquatic vs. semi-aquatic), placement in the catchment (soils, large lakes, ponds, large rivers, streams), and taphonomic histories (*in situ* preservation vs. secondary transport and winnowing). We find isotopic patterns that mirror those in modern catchments, which allow us to characterize the basin-scale hydrology of the ancient landscape, better constrain the region's paleoclimate, estimate paleoelevations of the Sevier orogenic belt, and identify the potential to refine habitat preference and migration patterns for paleobiologic studies.

GEOLOGIC SETTING

Exposures of the Two Medicine (TMF) and Judith River (JRF) Formations (Montana Group) span an ~300 km transect, encompassing both upstream and downstream portions of the Campanian foreland basin of Montana and Alberta (Fig. 1). Sediments preserved within these formations were shed from the Sevier fold-and-thrust belt and Cordilleran highlands to the west, transported by fluvial systems east-northeastward, and eventually deposited on alluvial plains, coastal plains, and into the epicontinental seaway of the Western Interior. The TMF contains fluvial sandstones of braided and meandering origin, a variety of interchannel facies including well-developed paleosol horizons, and rare, but widespread, occurrences of lacustrine intervals deposited in an up-dip alluvial plain (Rogers, 1998). Tectonic reconstructions place the TMF ~40 km to the east of the Sevier fold-and-thrust belt near Wolf Creek, Montana, and ~140 km at the U.S.-Canadian border (Price and Fermor, 1986; Sears, 2001). The JRF is dominated by coastal plain environments including tidally influenced fluvial sandstones, carbonaceous pond and backwater facies, paleosols displaying hydromorphic features, and shoreface sandstones, which directly interfinger with nearshore marine strata of the Western Interior Seaway (WIS) (Eberth and Hamblin, 1993; Rogers, 1998). The middle to upper portions of the TMF are time equivalent to the JRF based on

* Corresponding author. Current address: Department of Geology and Geophysics, University of Wyoming, Laramie, Wyoming 82071, USA, bforema1@uwyo.edu.

 0883-1351/11/0026-0545/$3.00

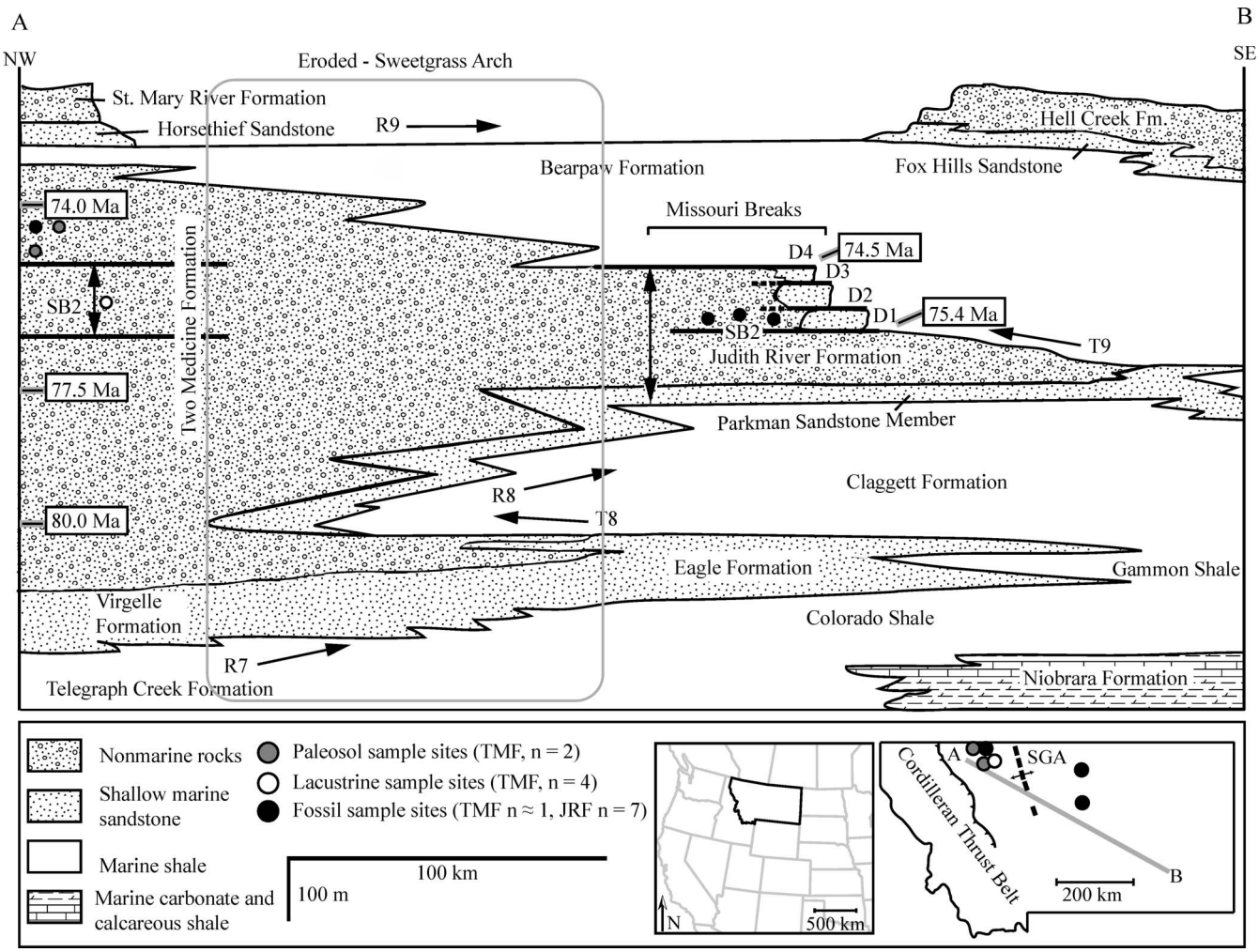

FIGURE 1—Schematic cross section of the Montana Group showing stratigraphic relationships of sample localities and correlation to major regressive-transgressive cycles of Kauffman (1977). Inset of maps of the western United States shows position of Montana and sample localities and transect position for cross section across the state (line A–B). SB2 = sequence boundary and D1–4 = parasequences identified by Rogers (1994, 1998); JRF = Judith River Formation; TMF = Two Medicine Formation; SGA = Sweetgrass Arch. Modified from Gill and Cobban (1973) and Rogers and Kidwell (2000). Radiometric ages for bentonite horizons from Foreman et al. (2008), Rogers et al. (1993), and Rogers and C.C. Swisher (unpublished data, 1996).

dated bentonite horizons (Rogers et al., 1993; Foreman et al., 2008); however, erosion over the Sweetgrass Arch has removed intervening strata (Fig. 1).

Sample Sites

Two Medicine Formation Sites.—Within the TMF type area an ~55-m-thick interval of lacustrine sediments crops out for ~15 km^2 through the drainage of the Two Medicine River, and is located ~230 m above a bentonite horizon dated at ~80 Ma (Rogers et al., 1993; Rogers, 1998). The lacustrine interval contains a basal carbonate-shale zone 10–20 m thick that underlies a zone of gray shales and minor sandstone beds. The carbonate beds range in thickness from 10 to 30 cm, but in some cases reach thicknesses of ~0.5 m. Carbonate layers are green, massive, and contain rare thromboids, charophytes, calcite vugs, occasional quartz grains, clay rip-ups, and chert stringers. The carbonate layers are interbedded with noncalcareous gray-green and purple massive shales and siltstones ranging in thickness from 10 cm to >1 m. The lacustrine interval is underlain and overlain by fluvial sandstones and paleosols throughout its extent.

Pedogenic carbonate samples are derived from paleosols directly above the lacustrine interval and from paleosols ~120 m stratigraphically higher and geographically ~35 km to the north (Fig. 1). TMF paleosol horizons are meter scale in thickness, red in color, mottled, and contain gray root traces. Pedogenic carbonate nodules derived from the paleosols range in diameter from 1 to 5 cm and were recovered *in situ* approximately 30 cm below the upper contact of the paleosol.

Approximately 50 meters below the Two Medicine Formation and Bearpaw Formation contact, an area of small fluvial sandstones, channel abandonment facies, and interchannel floodplain facies crops out near the U.S.-Canada border (Fig. 1). Fluvial sandstones are characteristically small in this area, typically 1–3 meters thick with traceable, lenticular margins. Siltstone lenses containing plant debris and burrows also crop out in the area. They are typically <1 m thick, extend laterally between 33 and 76 m, and lie laterally adjacent as well as conformably overlie cross-bedded sandstones (Rogers, 1990). We group all surface-collected fossil samples (unionid, gar, crocodile) from this area into a general stream environment because they cannot be unequivocally tied to either the small fluvial sandstone or channel abandonment facies.

Judith River Formation Sites.—Unionid bivalve shells, gar scales, and crocodile teeth recovered from the JRF were derived from microfossil bone bed sites hosted in fluvial and pond facies in the coastal plain along the margin of the Western Interior Seaway (Rogers and Kidwell, 2000). Fluvial sites are typically sheetlike in geometry (hundreds of

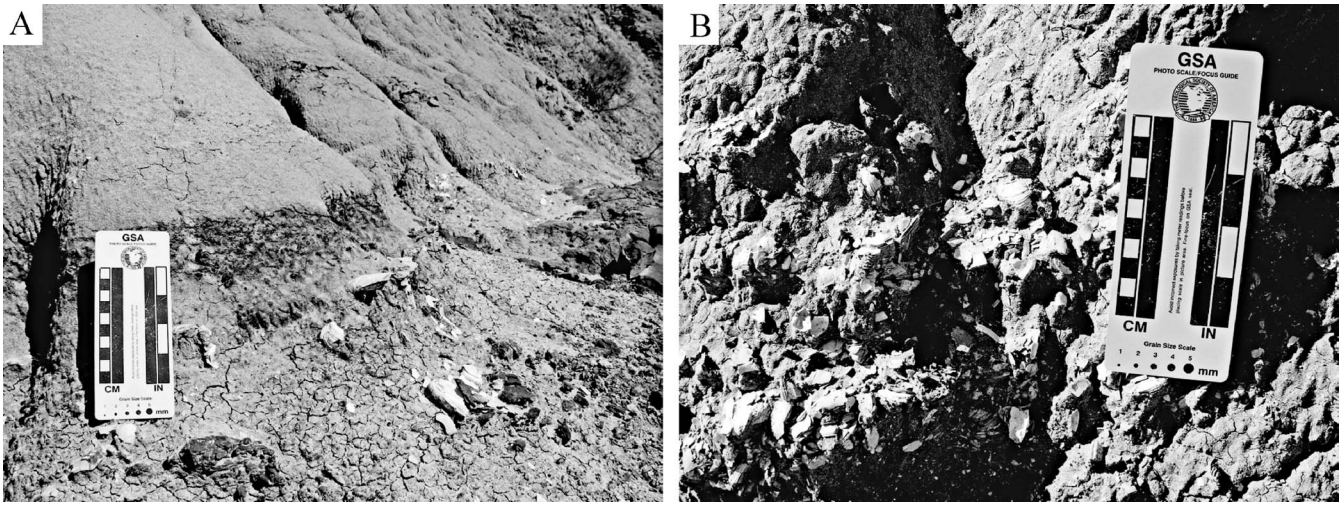

FIGURE 2—Representative fossils from the Judith River Formation. A) Fluvial-hosted unionid bivalve shells in life position. B) Pond-hosted unionid bivalve shell hash.

meters wide), 2.5–10 m thick, and multistoried. They are composed of gray, fine-grained sandstones with low-angle inclined sets, small- to medium-scale trough cross-bedding, and planar tabular cross-bed sets locally. Carbonaceous and clay drapes are common. Basal contacts are erosional and upper contacts are gradational or erosional. The multistoried nature and larger geometry of the JRF fluvial sand bodies, in comparison to the TMF stream facies, suggest that these were main thoroughfares for sediment in the basin and drained a greater catchment area (Leopold and Maddock, 1953; Mulder and Syvitski, 1996). Thus we view JRF fluvial facies and TMF stream facies as representing main stem and tributary rivers, respectively.

Unionid shells, gar scales, and crocodile teeth are found within lag deposits typically 10 cm thick (Rogers and Kidwell, 2000). Unionid shells analyzed in this study were predominantly recovered in life position (i.e., with articulated valves and evidence of only minor breakage and wear) (Fig. 2A). In contrast, vertebrate material recovered from fluvial scours shows evidence of transport (i.e., abrasion, rounding, polishing) not present in pond-hosted vertebrate fossils (Rogers and Brady, 2010). Rogers and Brady (2010) propose vertebrate sites hosted within these fluvial sandstones represent reworked and winnowed accumulations originally deposited in pond facies (i.e., parautochthonous or allochthonous deposits), rather than *in situ* concentrations formed within the fluvial channel itself. Supporting this claim are multiple outcrop exposures of fluvial channels scouring subjacent pond facies with vertebrate material clearly draped along scour surfaces and traceable into the fossil-rich pond facies (Rogers and Kidwell, 2000; Rogers and Brady, 2010). Moreover, early diagenetic uptake patterns of rare earth elements into fossil material are identical between fluvial and pond facies, indicating shared early fossilization conditions and history (Rogers et al., 2010).

Samples were also recovered from microfossil bone beds in gray tabular carbonaceous shales and silty claystones. The deposits are typically ~1 m thick and mostly massive in structure, although laminated carbonaceous debris is common. Contorted bedding is also present in some areas. Basal and upper contacts are commonly sharp. The sites can be traced in outcrop for over 100 m, and are interpreted as paralic ponds or lakes in coastal fluvial backwaters. Fossil material is typically dispersed and contains a variety of terrestrial and aquatic animal remains such as dinosaur, crocodiles, *Champsosaurus*, fish, turtles, and small freshwater invertebrates (e.g. *Sphaerium*), high-spired gastropods, and fragments of unionid bivalves (Fig. 2B). These are viewed as autochthonous, attritional fossil accumulations, which were concentrated due to relatively slow sedimentation rates in this quiet-water setting (Rogers and Brady, 2010).

METHODS

Prior to isotopic analyses, the mineralogy of carbonates and fossil material was determined using a PANalytical X'Pert PRO PW3040 x-ray diffractometer with a 2.2 kilowatt Cu-anode tube x-ray source. Samples were scanned from a start angle of 5°–65°, using a step size of 0.0167113°, time per step of 10.160 seconds, and scan speed of 0.208891° per second, with a total of 3590 steps run in a continuous scan mode. The program High-Score Plus (PANalytical Inc., www.panalytical.com) was used for background reduction and Kα2 stripping before identification of mineral phases (see Supplementary Data[1] for example spectrum and mineral identification).

Lacustrine and pedogenic carbonates were cut, polished, and their micritic cores sampled using a dental drill. Unionid bivalves were washed in distilled water multiple times and drilled vertically near the umbo of the shell. Aragonitic samples were roasted at 200 °C and reacted at ~77 °C with anhydrous phosphoric acid before introduction into a Finnigan MAT 253 triple-collector isotope ratio mass spectrometer at the University of Michigan. The ganoine from gar scales and enamel from crocodile teeth were also bulk sampled by drilling, avoiding dentine material. Approximately one mg was separated from each of the scales and teeth, soaked in 0.1 N acetic acid–calcium acetate buffered solution for 24 hours, rinsed in distilled water, and dried (methods after Koch et al., 1997). Samples were then powdered and reacted with dehydrated phosphoric acid under a vacuum (in the presence of Ag foil) before introduction to an automated carbonate preparation device (KIEL-III) coupled to the Finnigan MAT 252 mass spectrometer at 70 °C (University of Arizona) and 75 °C (University of Iowa). Oxygen and carbon isotope compositions reported are from the carbonate component of the hydroxyapatite. All analyses were normalized to international reference standards VPDB, VSMOW, NBS-19, NBS-18, and in-house standards. Results are reported in ‰ (VPDB) in standard δ notation, where $\delta = (R_{sample}/R_{standard} - 1)*1000‰$ and R is the ratio of $^{18}O/^{16}O$ or $^{13}C/^{12}C$ in the sample and standard. Precision for the analyses is better than 0.1‰. The data presented here consist of 120 new analyses supplemented with data from Fricke et al. (2008, 2009, 2010).

Estimating $\delta^{18}O$ of Water

In order to obtain and compare surface water $\delta^{18}O$ estimates from the different proxies, the temperature effects during carbonate

[1] palaios.ku.edu

TABLE 1—Equations used in this study to calculate surface water $\delta^{18}O$.

Equations	Reference
$\delta^{18}O_{shell}$ (VPDB) = 0.89 * $\delta^{18}O_{river\ water}$ (VSMOW) − 0.98	Kohn and Dettman (2007)
$\delta^{18}O$ (VSMOW) = 1.03091 * $\delta^{18}O$ (VPDB) + 30.91	Coplen et al. (1983)
1000 ln α = (2.78 *10^3) * T^{-2} − 2.89	Friedman and O'Neil (1977)
α = (1000 + $\delta^{18}O_{CO3}$ (VSMOW)) / (1000 + $\delta^{18}O_{H2O}$ (VSMOW))	
T = temperature in degrees Kelvin	

precipitation and biologic hard-part construction must be taken into account. We used the linear regression of Kohn and Dettman (2007) between unionid shell $\delta^{18}O$ and mean annual river water $\delta^{18}O$ to estimate ancient water values (Table 1). This relationship is robust across multiple modern unionid taxa and river temperatures as long as mean annual temperature is >10 °C, which was the case in the Campanian of Montana (Wolfe and Upchurch, 1987; Kohn and Dettman, 2007).

In estimating soil and lake water $\delta^{18}O$ we used Campanian paleofloral estimates of mean annual temperature (MAT; 16 °C) and mean warm month temperature (WMMT; 24 °C) in Montana from Wolfe and Upchurch (1987). Modern soil temperatures at depth show reduced seasonality and are typically ~2.5 °C warmer than MATs (Quade et al., 2007). Thus we calculated soil water $\delta^{18}O$ (VSMOW) at 18.5 °C (Friedman and O'Neil, 1977; Coplen et al., 1983) (Table 1). Lacustrine carbonate tends to form in the late spring and summer months as temperatures warm, thermocline development induces lake stratification, and increased photosynthetic activity induces supersaturation of calcium and carbonate ions within the epilimnion. Thus we used the WMMT of 24 °C as an estimate for lacustrine carbonate precipitation (Table 1). For both pedogenic and lacustrine carbonates an uncertainty in temperature assignment of 5 °C results in uncertainty in surface water $\delta^{18}O$ of ~1‰. Hence soil water and lake water estimates (within 0.4‰ of each other) should be viewed as indistinguishable given this uncertainty. Moreover, individual samples should be seen as multi-year averages (potentially up to hundreds of years for soil carbonates), given our bulk sampling approach.

Currently, the fractionation equation between oxygen isotopes in the carbonate component of hydroxyapatite and surface water (or body water) is unknown for gar scales and crocodile teeth; however, fish and crocodiles form the phosphate component of hydroxyapatite and otoliths (in fish) in isotopic equilibrium with ambient water (Kolodny et al., 1983; Patterson et al., 1993; Amiot et al., 2007). Although we cannot explicitly estimate surface water $\delta^{18}O$ from these samples, the variability within a given proxy (i.e., gar to gar, and crocodile to crocodile) should reflect variability in water $\delta^{18}O$ values rather than temperature because gar experience optimum growth at warmer temperatures (>26 °C) and crocodiles employ thermoregulatory behaviors to maintain warmer body temperatures (Coutant, 1977; Smith, 1979; Wismer and Christie, 1987). Thus gar and crocodile records will probably reflect warm month water $\delta^{18}O$ values, whereas unionid shells will reflect year-round mean water $\delta^{18}O$ values.

RESULTS

Diagenetic Assessment

Isotopic compositions of the proxies are interpreted to be largely unaltered. Thin sections of lacustrine carbonates and pedogenic carbonate nodules have a microcrystalline texture of micron-sized, interlocking, equant calcite crystals, a mineralogy confirmed using x-ray diffractometry, and indicate that minimal recrystallization occurred. X-ray diffraction of the unionid bivalves indicates they are composed of aragonite (>99%). Shells display a mother-of-pearl luster and well-preserved growth laminae. Gar scales, crocodile teeth, and hadrosaur teeth are also inferred to record primary isotopic signals, as they are closely associated (within centimeters in some cases) with primary aragonitic bivalves. Ganoine and enamel from scales and teeth are more diagenetically stable than the aragonite shells owing to larger size and denser packing of crystals as well as the reduced percentage of organic components in the hydroxyapatites (Nelson et al., 1986; Kohn and Cerling, 2002). Thus it seems unlikely that the aragonite would remain unaltered whereas the enamel and ganoine would be altered. Fricke et al. (2008) provide a detailed diagenetic evaluation of Campanian fossil sites in the Two Medicine, Judith River, and Dinosaur Park Formations, which partially overlap with sites studied here. They examined stable isotope compositions from gar scales, dinosaur teeth, and authigenic minerals, and concluded the taxonomic offsets, enamel versus dentine isotopic values, and mineralogy indicated preservation of primary isotopic signals (Fricke et al., 2008).

Isotopic Results

Values of $\delta^{18}O$ and $\delta^{13}C$ segregate carbonate sediments and biogenic hard parts by depositional environment and by geographic position in the foreland basin (Figs. 3A–B). Values for individual samples can be found in the Supplementary Data[1]. Mean $\delta^{18}O$ and $\delta^{13}C$ values for the different proxies and environments are provided in Table 2. Pedogenic and lacustrine carbonate values substantially overlap (Fig. 3A). A two-tailed t-test cannot distinguish between the two populations for $\delta^{13}C$ values (p-value = 0.82), but can for $\delta^{18}O$ values (p-value = 0.02); however, this statistical difference does not account for temperature uncertainties or variability during calcite precipitation, meaning the two groups should be considered equivalent. Bivalve shells fall into three groups based on $\delta^{18}O$ and $\delta^{13}C$ values (Fig. 3A, Table 2). Unionid bivalves in Group 1 are derived from the fluvial sandstones and some coastal ponds of the JRF, with one outlier from the TMF stream facies. Two of the unionid bivalves in Group 2 are from coastal ponds of the JRF and one is from large fluvial sandstones of the JRF. Unionid bivalves from Group 3 are only found in stream facies of the TMF and coastal ponds of the JRF. These groupings are statistically significant based on single factor ANOVA for both $\delta^{18}O$ and $\delta^{13}C$ (p-value $\ll$ 0.05). Overall the quiet-water facies (ponds, lakes, soils) are characterized by higher $\delta^{18}O$ values and lower $\delta^{13}C$ values than large fluvial facies. Lakes and soil carbonates are characterized by slightly lower $\delta^{18}O$ values from Group 3 unionids, but substantially lower $\delta^{13}C$ values from both fluvial and pond unionids.

Gar scales and crocodile teeth display a wide range of stable isotope compositions, but segregate by the geologic formation of origin (Fig. 3B). Mean values are shown in Table 2. The results show a proximal-to-distal pattern in $\delta^{18}O$ and $\delta^{13}C$ values, with both gar and crocodile material displaying lower values in the up-dip alluvial plain of the TMF. Two-tailed t-tests support the isotopic offset between the formations for both $\delta^{18}O$ and $\delta^{13}C$ values of gar scales and crocodile teeth (p-values $\ll$ 0.05). Unlike the unionid data sets, gar scales obtained from different facies in the JRF (pond and large river) do not display substantially different values (Fig. 3B), and a two-tailed t-test cannot distinguish between pond and fluvial gar-scale data sets (p-value = 0.28 for $\delta^{18}O$ values; p-value = 0.86 for $\delta^{13}C$ values).

Mean water estimates for the unionid groupings are presented in Table 2 and individual sample estimates in the Supplementary Data[1]. The surface water estimates represent multi-year means, as our bulk sampling method mixes material from multiple shell annuli (Dettman et al., 1999).

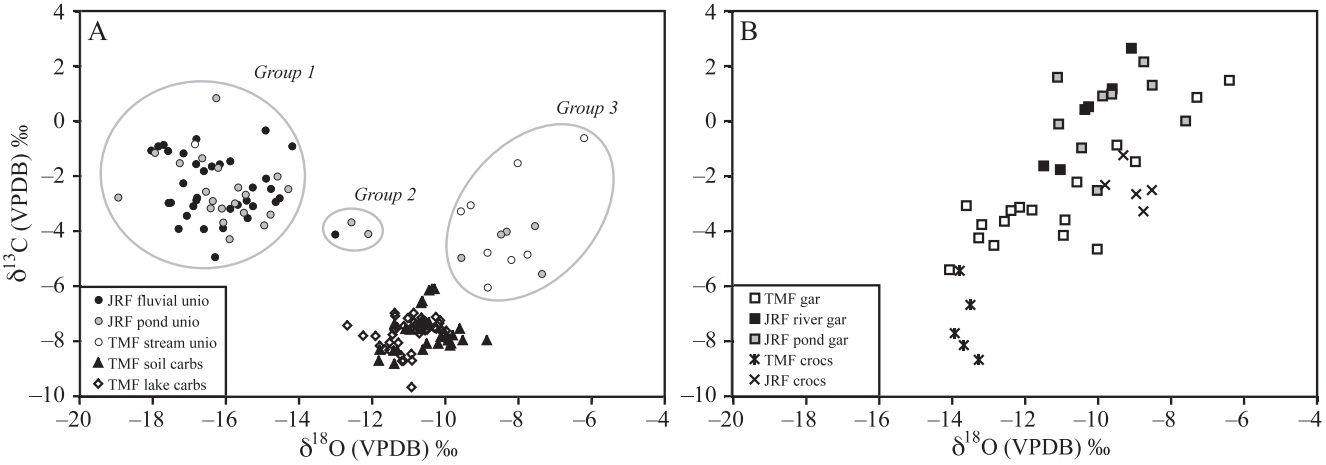

FIGURE 3—Bivariate plots of $\delta^{18}O$ versus $\delta^{13}C$. A) Unionid shell (unio), pedogenic carbonate, and lacustrine data (carbs). B) Gar scales and crocodile teeth (crocs) data. JRF = Judith River Formation; TMF = Two Medicine Formation.

CATCHMENT STRUCTURE

Within our sedimentologic framework, isotopic patterns from authigenic carbonates and unionid shells mimic those found within modern catchments. The $\delta^{18}O$ value of river water represents an amount-weighted mean of precipitation across modern catchments (Dutton et al., 2005). River water is negatively offset from local precipitation due to runoff contributions from higher elevations, yet the smaller the catchment the more closely river water $\delta^{18}O$ values match local precipitation $\delta^{18}O$ values (Garzione et al., 2000; Dutton et al., 2005; Rowley and Garzione, 2007). This is consistent with the $\delta^{18}O$ offset between the main stem rivers and streams in our study. Lake and pond water $\delta^{18}O$ values in modern catchments are heavily dependent on the hydrologic input (i.e., direct rainfall, fluvial, or groundwater) and the degree of evaporation, which leads to higher $\delta^{18}O$ values (Talbot, 1990). In our study the similarity between soil water, typically taken as a close approximation of meteoric rainfall (Cerling and Quade, 1993), and pond or lake water suggests a local, low-elevation rainfall source with minimal fluvial input and evaporation. Pond unionid shells that fall into Group 1 (Fig. 3A) likely reflect periods when fluvial systems were in direct communication with ponds and inundated pond water subsuming their isotopic signature.

Values of $\delta^{13}C$ also mimic modern catchment patterns. The $\delta^{13}C$ value of dissolved inorganic carbon (DIC) in river water typically shows a downstream shift toward lower values as vegetation becomes denser and weatherable carbonate rock exposures rarer (Aucour et al., 1999; Yang et al., 1996). Moreover, water bodies with turbulent and fast flows typically display higher $\delta^{13}C$ DIC values than stagnant water due to increased outgassing and reduced respiration of organic matter in the former (Finlay et al., 1999). Indeed these are the general $\delta^{13}C$ patterns observed in our isotopic records (Figs. 3A–B). Although the specific biologic effects on carbon isotope fractionation are unknown in modern unionids, shell $\delta^{13}C$ values generally correlate with DIC (Dettman et al., 1999). The $\delta^{13}C$ values in our study indicate a greater proportion of respired organic matter in ponds as compared to rivers (Fig. 3A). Lake and soil carbonates display the lowest $\delta^{13}C$ values of the environments sampled and are consistent with an exclusively degraded organic matter source to water DIC.

Gar and crocodile records show a different pattern, and there are two potential explanations for the discrepancy. Gar and crocodiles may have moved among different portions of the fluvial system, coastal ponds, and even the Western Interior Seaway during growth, thereby spatially averaging the respective isotopic signatures of these environments. In this case, the proximal-distal gradient reflects that gar and crocodile in the TMF are not migrating to the seaway and incorporating its higher $\delta^{18}O$ and $\delta^{13}C$ signature, which is consistent with the typical modern geographic ranges of the taxa (e.g., Hutton, 1989; Snedden et al., 1999). Moreover, it implies that this biologic filter has eliminated primary, *in situ* environmental isotopic variability, which should be kept in mind when these proxies are used for climatic or elevation reconstructions. The second explanation attributes the isotopic patterns to the season of scale and tooth growth, with no movement between environments. Because there will be minimal difference in the temperature of scale and tooth growth in the two geographic areas, as explained above, the proximal-distal gradient in the foreland basin may reflect a gradient in precipitation $\delta^{18}O$ values, potentially due to monsoons or elevation differences (discussed further below). This second case invokes the allochthonous taphonomic history of fluvially hosted vertebrate material (Rogers and Brady, 2010) to explain why gar scales do not show the same isotopic offset between JRF river and pond environments observed in autochthonous unionid shell records from the two environments.

TABLE 2—Summary statistics of isotope data. JRF = Judith River Formation; TMF = Two Medicine Formation.

Samples	Mean $\delta^{18}O$ ‰ (VPDB)	One std. dev.	Mean water $\delta^{18}O$ ‰ (VSMOW)	One std. dev.	Mean $\delta^{13}C$ ‰ (VPDB)	One std. dev.
Unionid shells (Group 1) (n = 54)	−16.5	2.5	−17.1	2.7	−2.4	1.1
Unionid shells (Group 2) (n = 3)	−12.6	0.5	−13.0	0.5	−3.9	0.3
Unionid shells (Group 3) (n = 13)	−8.3	1.0	−8.2	1.1	−3.9	1.6
Pedogenic carbonate (n = 25)	−10.5	0.8	−9.5	0.8	−7.7	0.8
Lacustrine carbonate (n = 47)	−10.9	0.6	−9.1	0.6	−7.7	0.5
TMF gar scales (n = 17)	−11.2	2.2	N/A	N/A	−2.8	1.9
JRF gar scales (n = 15)	−9.9	1.1	N/A	N/A	0.4	1.5
TMF crocodile teeth (n = 5)	−13.6	0.3	N/A	N/A	−7.3	1.3
JRF crocodile teeth (n = 5)	−9.1	0.5	N/A	N/A	−2.4	0.7

DISCUSSION

Paleoclimatic Implications

The paleoclimate of the Campanian foreland basin of Montana is characterized by a humid coastal plain (JRF) and a semi-arid, up-dip alluvial plain (TMF). The JRF contains abundant carbonaceous material, hydromorphic paleosols, and pollen taxa indicative of humid conditions (Jerzykiewicz and Sweet, 1987, 1988; Rogers, 1998). The semi-arid TMF contains depauperate palynological assemblages, drought-related death assemblages of dinosaurs, growth interruptions in conifer remains, and carbonate-bearing paleosols (Jerzykiewicz and Sweet, 1987, 1988; Rogers, 1990; Falcon-Lang, 2003). Furthermore, alternation between carbonate and shale deposition within the lacustrine deposits suggests seasonality in temperature and precipitation (Fig. 4).

Our isotopic results do not contradict the above climatic conditions, although we do not find evidence of excessive evaporative conditions in the Two Medicine Formation. We do not observe covariation in $\delta^{18}O$ and $\delta^{13}C$ values within the lacustrine samples, which commonly occurs in closed lake systems under evaporative conditions (Fig. 4; Talbot, 1990), nor are pedogenic carbonate $\delta^{13}C$ values consistent with water-stressed vegetation. Typical modern soil carbonate $\delta^{13}C$ values in areas dominated by C_3 vegetation fall between −9‰ and −15‰ (VPDB) (Cerling and Quade, 1993; Koch, 1998), but aridity causes $\delta^{13}C$ in vegetation to shift to higher values as plants keep their stomata closed for longer periods of time, decreasing the discrimination against ^{13}C and leading to higher pedogenic carbonate $\delta^{13}C$ values (e.g., Farquhar et al., 1989). While our pedogenic carbonates display higher values on average (−7.8‰), this value likely reflects the fact that the $\delta^{13}C$ value of the Cretaceous atmosphere was 1‰–2‰ higher than that of modern Earth rather than an evaporation signal (Barrera and Savin, 1999; Hasegawa et al., 2003).

Furthermore, soil water $\delta^{18}O$ estimates fall within the predicted range for the paleolatitude of the TMF. Using the empirical relationship of Dutton et al. (2005) relating the $\delta^{18}O$ of precipitation to latitude and an estimated paleolatitude of ~54° N for the sample sites (Besse and Courtillot, 2002), we obtain an estimate of −9.8‰ (VSMOW) for local precipitation. Adding a correction of −1.2‰ to account for lower $\delta^{18}O$ value for Cretaceous seawater compared to modern (Shackleton and Kennett, 1975) yields an estimate of −11.0‰. Substantial evaporation would display a positive offset from these predicted values, yet our estimates from pedogenic carbonates fall within this range, −10.5‰ ± 0.8‰ (VSMOW). The positive offset between pond/stream and soil/lake-water $\delta^{18}O$ values, however, could potentially reflect evaporation from these smaller water bodies. Alternatively, it could reflect seasonal difference in the $\delta^{18}O$ of rainfall, with lake and soil water recording lower $\delta^{18}O$ values associated with enhanced, potentially monsoonal, summer precipitation.

Fricke et al. (2010) proposed a strong monsoon operating within the Western Interior during the Campanian, with vapor masses moving westward across the foreland basin toward the Sevier orogenic belt, based on an atmospheric circulation model and isotopic records. Similar to their isotopic record, we observe a bimodal $\delta^{18}O$ pattern between quiet-water facies and trunk river facies, indicating high elevations sufficient to drive convective circulation. Whereas unionid shell records show no proximal-to-distal geographic pattern, however, authigenic carbonates, gar, and crocodile records show a distinct shift to lower $\delta^{18}O$ in basin-proximal sample sites. Assuming this signal is related to environmental variability (i.e., not due to biologic movement among environments), there are three possible causes for this pattern. The first is the continent effect, wherein vapor masses become progressively enriched in ^{16}O as they move inland and ^{18}O is preferentially incorporated into the condensate (Rozanski et al., 1993). Across modern landmasses this effect is roughly 1.5‰–2.0‰ per 1000 km (Rozanski et al., 1993). For the relatively narrow (300 km) foreland basin, however, this can only account for approximately 0.45‰–0.6‰ of the proximal-distal offset.

A difference in elevation could also account for the proximal-distal offset, as vapor masses are deflected to higher altitudes and Rayleigh distillation occurs (Dansgaard, 1964; Rozanski et al., 1993; Rowley, 2007). We can independently estimate the elevation difference using typical slopes for modern alluvial rivers. The steepest, gravel-dominated braided rivers have slopes on the order of 10^{-3} (Church, 2006), and projecting this across the foreland basin results in an elevation difference of 300 m between the TMF and JRF. This value is an upper estimate of elevation, as typical TMF and JRF rivers carried fine- to medium-grained sand and were more likely to be meandering than braided in planform (Rogers, 1998). By applying the lapse rate of Dutton et al. (2005) to this elevation difference we can account for only 0.87‰ of the proximal-to-distal offset. Thus neither continentality nor elevation is sufficient to explain the offset. Furthermore, it is difficult to explain why the offset would be different for the different proxies and not uniform among them. For ponds to lakes it is 2.2‰, for gar scales, 1.3‰, and for crocodiles, 4.5‰.

The third potential cause is the amount effect of Rozanski et al. (1993), typically observed in monsoon-dominated systems, wherein there is an inverse relationship between the $\delta^{18}O$ of precipitation and the amount of precipitation rained out in a region. In this scenario summer monsoonal precipitation across the foreland basin will be enriched in ^{16}O yielding lower $\delta^{18}O$ values in authigenic carbonate, gar, and crocodile records, all of which are growth-biased toward warmer months. The differential offsets among the proxies reflect different optimum growth periods and thermoregulatory behaviors during the late spring and summer months. The lack of a proximal-distal gradient in unionid shell $\delta^{18}O$ values reflects a yearly uniform mean value in proximal and distal locations, a feature observed in the Southeast Asian monsoon system (Araguás-Araguás et al., 1998). In future studies this hypothesis will be further tested using seasonal microsampling of the unionid shell material.

Paleoelevation Implications

Many studies have relied upon $\delta^{18}O$ values to reconstruct ancient topographies and identify the timing of uplift in major orogenic belts (Chamberlain and Poage, 2000; Garzione et al., 2000, 2006; Rowley and Garzione, 2007). In North America this method has been applied mostly to orogenic systems where atmospheric circulation patterns are well constrained and there is a single, dominant vapor source for precipitation such as in the Basin and Range (Horton and Chamberlain, 2006), Sierra Nevada (Mulch et al., 2006), and Cascades (Kohn et al., 2002). Similar paleoaltimetry studies are limited within the Western Interior during the Late Cretaceous because of uncertainties associated with the trajectories of frontal systems across foreland basins and air mass mixing from Gulf of Mexico, polar, and Pacific sources. Constraining these precipitation and circulation patterns is further complicated due to temporal fluctuations in the geographic extent of the seaway and topographic modification due to Sevier or Laramide uplift events. These uncertainties have been partially overcome recently by comparing proxy-derived isotopic records with modern spatial patterns in precipitation $\delta^{18}O$ values and paleoatmospheric circulation models (Kent-Corson et al., 2006; Fan and Dettman, 2009; Poulsen et al., 2007; Fricke et al., 2010).

While there are many elevation lapse rates presented in the literature (Rowley, 2007 and references therein), we use a lapse rate of −2.9‰/km from Dutton et al. (2005), based on meteoric $\delta^{18}O$ patterns in North America. The $\delta^{18}O$ offset between pond and trunk river water is 8.9‰, yielding an estimate of 3.1 km for the hypsometric mean elevation of the foreland basin's catchment, including the Sevier orogenic belt. Couched within this estimate are a number of assumptions, however. First, we assume that pond $\delta^{18}O$ values are representative of local

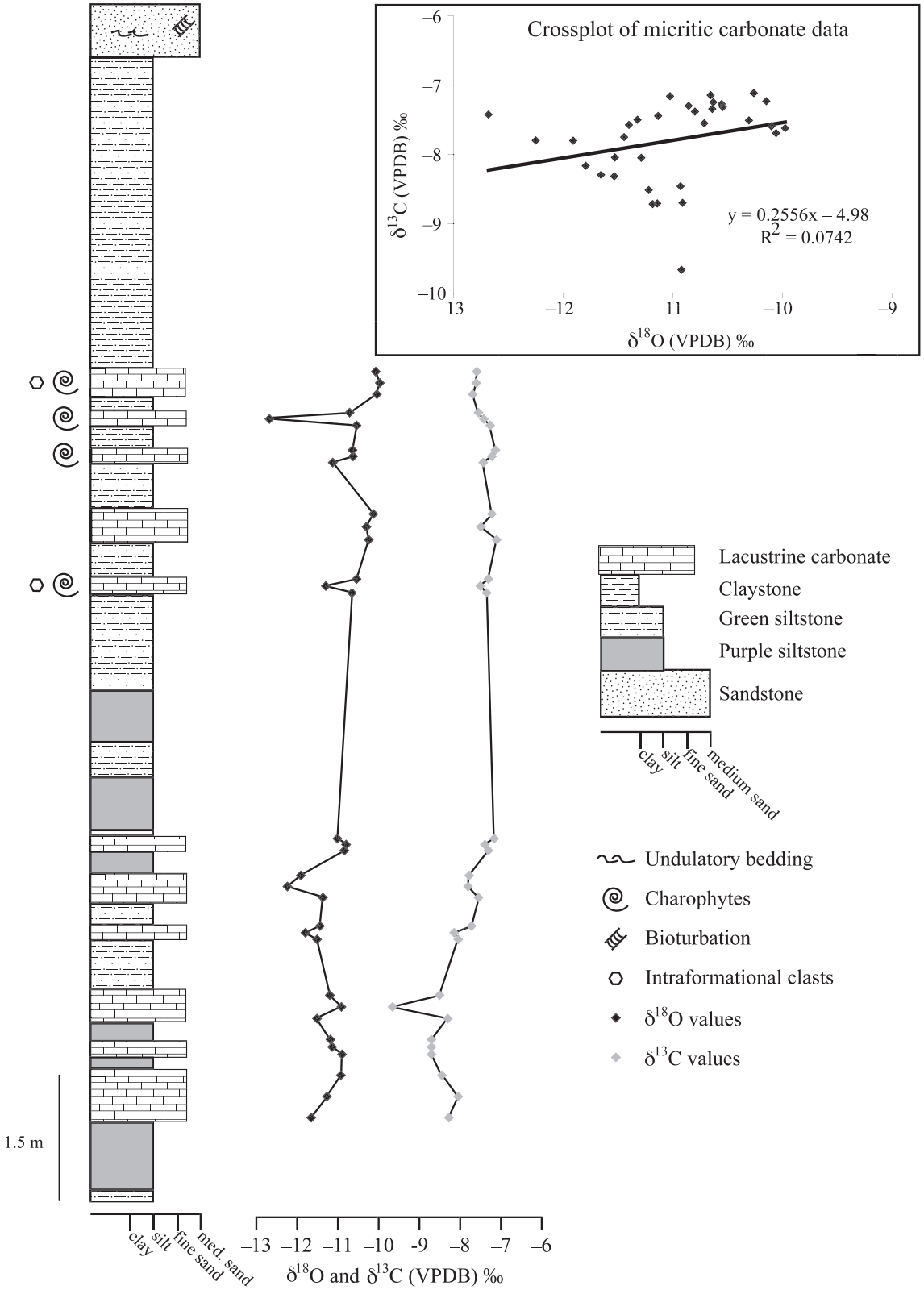

FIGURE 4—Stratigraphic section through lacustrine carbonate interval of Two Medicine Formation showing secular patterns in $\delta^{18}O$ and $\delta^{13}C$. Inset of $\delta^{18}O$ versus $\delta^{13}C$ bivariate plot of lacustrine data shows little covariation, suggesting a hydrologically open lake system.

precipitation and not evaporatively enriched in ^{18}O. If instead we use soil carbonates in estimating local precipitation $\delta^{18}O$ values (−9.5‰ VSMOW), as is typical of many studies, an estimate of 2.6 km is obtained. Thus, there could be a 0.5 km difference or ~16% additional uncertainty in elevation estimates depending on whether or not multiple proxies were sampled and analyzed. Furthermore, the main stem rivers undoubtedly received water from local precipitation and tributary streams as they flowed across the foreland basin on the way to empty

into the seaway, which would have diluted the high-altitude runoff $\delta^{18}O$ signal.

There remains a large offset between quiet-water facies and fluvial facies even in the coastal JRF, however, which is uncommon within modern landscapes (Dutton et al., 2005). This observation requires that: (1) the vast majority of fluvial water was derived from precipitation at or above ~2.6 km, (2) the $\delta^{18}O$ value of fluvial water was substantially lower ($\ll -17.1‰$) when it first entered the foreland basin, or (3) fluvial waters obtained a large fraction of their water from runoff during ^{16}O-enriched, monsoonal precipitation in the basin. We cannot explicitly exclude any of the three; however, the first scenario simply requires strong, asymmetric orographic precipitation focused on the eastern slope of the Sevier orogenic belt displaced from the central drainage divide. This precipitation pattern is common to modern large orogenic systems (i.e., those >40 km wide and 1.5 km high; Roe, 2005), and is broadly supported by the Campanian circulation models of Fricke et al. (2010). If instead fluvial water $\delta^{18}O$ values were substantially lower when they first entered the foreland basin, either the mean elevation of the Sevier orogenic belt was unrealistically high (i.e., equal to or greater than the modern Tibetan plateau) or rivers partially obtained water from a Pacific air mass source. Mid-Cretaceous circulation models of Poulsen et al. (2007), which incorporate a water isotope module into rainfall patterns, indicate exceedingly negative precipitation $\delta^{18}O$ values in the Sevier orogenic belt as Pacific air masses moved eastward. These air masses may have traveled across the drainage divide and rained out highly ^{16}O-enriched precipitation, or alternatively, rivers may have tapped far into the orogenic belt, similar to drainage systems for some Laramide lake systems, to obtain an exceptionally low $\delta^{18}O$ value (Carroll et al., 2008; Davis et al., 2008; Doebbert et al., 2010). Finally, if circulation models are correct and an active monsoon was operating within the Western Interior, seasonal variation in $\delta^{18}O$ was likely strong. For example, the modern Indian monsoon causes 9‰ seasonal fluctuation in New Delhi (Rowley, 2007). Indeed, Poulsen et al. 's (2007) circulation model suggests that 2‰–3‰ of precipitation $\delta^{18}O$ values are caused by the amount effect associated with large precipitation events. The offset between JRF coastal ponds and TMF lake and soil water falls within this range (2.2‰) and is consistent with the seasonal bias in the samples, i.e., lake and soil water derived from the summer months during the monsoon, whereas unionid shells in ponds record a multiyear average $\delta^{18}O$ of pond water spanning both monsoonal and non-monsoonal precipitation events. If foreland basin river systems had longer residence times, a portion of these low $\delta^{18}O$ values could be related to monsoonal precipitation rather than representing an elevation signal (Rowley, 2007).

Paleobiology

Modern organisms show distinct patterns in $\delta^{18}O$, $\delta^{13}C$, $\delta^{15}N$, and other isotopic systems that correlate with the environmental setting they inhabit (e.g., terrestrial, freshwater aquatic, estuarine, marine aquatic; Kelly, 2000; Clementz and Koch, 2001). These patterns are exploited in the fossil record to determine the habitat preferences of taxa without extant relatives or analogues, identify paleoniche partitioning, and track evolutionary transitions within a taxonomic group among habitats (Koch et al., 1998; Clementz et al., 2006, 2009; Morgan et al., 2009; Amiot et al., 2010). The results from our study indicate that it is possible to further subdivide freshwater settings and ecosystems for more resolved determinations of habitat preference if a wide range of depositional environments and sessile, autochthonous isotopic records (i.e., authigenic carbonates and unionid shells) are targeted for sampling.

Within the paleocatchment framework it should be possible to determine if and to what degree aquatic and semi-aquatic organisms are visiting the different freshwater sub-environments either seasonally or through ontogeny by sub-sampling biominerals along growth structures. For example, Fricke et al. (2009) find a proximal-distal offset in $\delta^{18}O$ and $\delta^{13}C$ values (3.3‰ and 3.2‰, respectively) of hadrosaurid dinosaur tooth enamel across the Campanian foreland basin of Montana as well as further south across Utah and New Mexico. They argue against seasonal, long-distance migration within the foreland basin for nesting or feeding purposes, as hypothesized by previous authors (e.g., Horner and Makela, 1979). If migration were common the two sampling areas would show a more bimodal distribution of $\delta^{18}O$ and $\delta^{13}C$ values with a portion of TMF hadrosaur teeth displaying JRF-type values and vice versa. Fricke et al. (2009) argue that the proximal-distal offset must be due to different environmental conditions in the upland and lowland regions of the foreland basins. Here, we have argued against elevation and continental effects on $\delta^{18}O$ values within the basin using independent sedimentologic data and have shown similar multi-year mean values in surface-water conditions in the two portions of the foreland basin with bulk-sampled unionid shells. Thus, only two hypotheses remain to explain the proximal-distal offset: (1) the isotopic difference between upland and lowland hadrosaur tooth enamel is seasonal in nature and related to the monsoon; or (2) hadrosaurs were preferentially living closer to fluvial channels in the TMF, where $\delta^{18}O$ and $\delta^{13}C$ environmental values would be lower, to avoid semi-arid conditions of the floodplain. Currently we favor a monsoonal cause because these samples are associated with small streams and ponds and the offset is consistent among multiple proxies (i.e., hadrosaurs, gar scales, and crocodile teeth). Future work subsampling tooth enamel, scale ganoine, and shell material will better resolve the seasonal variability in $\delta^{18}O$ values of precipitation. If hadrosaur, gar, and crocodile values are truly a seasonal signal, they should be cyclical in nature rather than punctuated events (Stanton Thomas and Carlson, 2004).

CONCLUSIONS

This study integrated stable isotope records with alluvial architecture, sedimentology, and taphonomy. Our multi–depositional environment and multi-proxy approach allowed us to reconstruct the major components of the catchment structure within the Campanian foreland basin of Montana. We document nearly uniform multi-year average $\delta^{18}O$ values across the 300 km basin; however, proxy records with a summer growth bias show a distinct shift toward lower $\delta^{18}O$ values in the proximal portions of the basin. This proximal-distal gradient is consistent with hypotheses asserting the strong dominance of monsoonal precipitation in the Western Interior. Moreover, we document an extremely negative $\delta^{18}O$ signal imparted to large, main stem rivers by runoff from high elevation in the Sevier orogenic belt. The proximal-distal pattern is only apparent when all major components of the catchment are sampled and we show how some proxies may not capture the full isotopic range of variability, due not only to biologic behaviors, but also taphonomic history. While biologic behavior and isotopic fractionation patterns have been consistently taken into account in the literature (see e.g., Koch, 1998; Kohn and Dettman, 2007 and references therein), taphonomic history (with the exception of diagenetic history) and alluvial architecture are more rarely considered, although their incorporation may lend important, independent support for paleoclimatic and paleoelevation reconstructions.

ACKNOWLEDGMENTS

This study was financially supported by a Scott Turner Research Grant (2006) from the University of Michigan and a Geological Society of America Research Grant (2007) to B.Z.F. It was completed under a National Science Foundation Graduate Research Fellowship to B.Z.F. Thanks to R. Wellman, J. Wellman, and R. Regan for land access, and L. Wingate, P.D. Gingerich, M. D'Emic, M. Brady, E. Hajek, and K. Robinson for lab and field assistance as well as discussions that

benefited this manuscript. We also thank Andreas Mulch and an anonymous reviewer for their comments.

REFERENCES

Amiot, R., Buffetau, E., Lécuyer, C., Wang, X., Boudad, L., Ding, Z., Fourel, F., Hutt, S., Martineau, F., Medeiros, M.A., Mo, J., Simon, L., Suteethorn, V., Sweetman, S., Tong, H., Zhang, F., and Zhou, Z., 2010, Oxygen isotope evidence for semi-aquatic habits among spinosaurid theropods: Geology, v. 38, p. 139–142.

Amiot, R., Lécuyer, C., Escarguel, G., Billon-Bruyat, J.-P., Buffetau, E., Langlois, C., Martin, S., Martineau, F., and Mazin, J.-M., 2007, Oxygen isotope fractionation between crocodilian phosphate and water: Palaeogeography, Palaeoclimatology, Palaeoecology, v. 243, p. 412–420.

Araguás-Araguás, L., Froehlich, K., and Rozanski, K., 1998, Stable isotope composition of precipitation over Southeast Asia: Journal of Geophysical Research: Atmospheres, v. 103, p. 28,721–28,742.

Aucour, A.-M., Sheppard, S.M.F., Guyomar, O., and Wattelet, J., 1999, Use of ^{13}C to trace origin and cycling of inorganic carbon in the Rhône river system: Chemical Geology, v. 159, p. 87–105.

Barrera, E., and Savin, S.M., 1999, Evolution of late Campanian–Maastrichtian marine climates and oceans, *in* Barrera, E., and Johnson, C.C., eds., Evolution of the Cretaceous Ocean-Climate System: Geological Society of America Special Paper, Boulder, Colorado, v. 332, p. 245–282.

Besse, J., and Courtillot, V., 2002, Apparent and true polar wander and the geometry of the geomagnetic field over the last 200 Myr: Journal of Geophysical Research, v. 107, p. 2300–2331.

Carroll, A.R., Doebbert, A.C., Booth, A.L., Chamberlain, C.P., Rhodes-Carson, M.K., Smith, M.E., Johnson, C.M., and Beard, B.L. 2008, Capture of high-altitude precipitation by a low-altitude Eocene lake, western U.S.: Geology, v. 36, p. 791–794.

Cerling, T.E., and Quade, J., 1993, Stable carbon and oxygen isotopes in soil carbonates, *in* Swart, P.K., Lohmann, K.C., McKenzie, J., and Savin, S., eds., Climate Change in Continental Isotopic Records: Geophysical Monograph 78, American Geophysical Union, Washington, D.C., p. 217–231.

Chamberlain, C.P., and Poage, M.A., 2000. Reconstructing the paleotopography of mountain belts from the isotopic composition of authigenic minerals: Geology, v. 28, p. 115–118.

Church, M., 2006, Bed material transport and the morphology of alluvial river channels: Annual Review of Earth and Planetary Science, v. 34, p. 325–254.

Clementz, M.T., Goswami, A., Gingerich, P.D., and Koch, P.L., 2006, Isotopic records from early whales and sea cows: Contrasting patterns of ecological transition: Journal of Vertebrate Paleontology, v. 26, p. 355–370.

Clementz, M.T., and Koch, P.L., 2001, Differentiating aquatic mammal habitat and foraging ecology with stable isotopes in tooth enamel: Oecologia, v. 129, p. 461–472.

Clementz, M.T., Sorbi, S., and Domning, D.P., 2009, Evidence of Cenozoic environmental and ecological change from stable isotope analysis of sirenian remains from the Tethys-Mediterranean region: Geology, v. 37, p. 307–310.

Coplen, T.B., Kendall, C., and Hopple, J., 1983, Comparison of stable isotope reference samples: Nature, v. 302, p. 236–238.

Coutant, C. C., 1977, Compilation of temperature preference data: Journal of Fisheries Research Board of Canada, v. 34, p. 739–745.

Dansgaard, W., 1964, Stable isotopes in precipitation: Tellus, v. 16, p. 436–468.

Davis, S.J., Wiegand, B.A., Carroll, A.R., and Chamberlain, C.P., 2008, The effect of drainage reorganization on paleoaltimetry studies: An example from the Paleogene Laramide foreland: Earth and Planetary Science Letters, v. 275, p. 258–268.

Dettman, D.L., Reische, A.K., and Lohmann, K.C., 1999, Controls on the stable isotope composition of seasonal growth bands in aragonitic fresh-water bivalves (Unionidae): Geochimica et Cosmochimica Acta, v. 63, p. 1049–1057.

Doebbert, A.C., Carroll, A.R., Mulch, A., Chetel, L.M., and Chamberlain, C.P., 2010, Geomorphic controls on lacustrine isotopic compositions: Evidence from the Laney Member, Green River Formation, Wyoming: Geological Society of America Bulletin, v. 122, p. 236–252.

Dutton, A.D., Wilkinson, B.H., Welker, J.M., Bowen, G.J., and Lohmann, K.C., 2005, Spatial distribution and seasonal variation in $^{18}O/^{16}O$ of modern precipitation and river water across the conterminous USA: Hydrological Processes, v. 19, p. 4121–4146.

Eberth, D.A., and Hamblin, A.P., 1993, Tectonic, stratigraphic, and sedimentologic significance of a regional discontinuity in the upper Judith River Group (Belly River wedge) of southern Alberta, Saskatchewan, and northern Montana: Canadian Journal of Earth Science, v. 30, p. 174–200.

Falcon-Lang, H.J., 2003, Growth interruptions in silicified conifer woods from the Upper Cretaceous Two Medicine Formation, Montana, USA: Implications for palaeoclimate and dinosaur palaeocology: Palaeogeography, Palaeoclimatology, Palaeoecology, v. 199, p. 299–314.

Fan, M., and Dettman, D.L., 2009, Late Paleocene high Laramide ranges in northeast Wyoming: Oxygen isotope study of ancient river water: Earth and Planetary Science Letters, v. 286, p. 110–121.

Farquhar, G.D., Ehleringer, J.R., and Hubick, K.T., 1989, Carbon isotope discrimination and photosynthesis: Annual Review of Plant Physiology and Plant Molecular Biology, v. 40, p. 503–537.

Finlay, J.C., Power, M.E., and Cabana, G., 1999, Effects of water velocity on algal carbon isotope ratios: Implications for river food web studies: Limnology and Oceanography, v. 44, p. 1198–1203.

Foreman, B.Z., Rogers, R.R., Deino, A.L., Wirth, K.R., and Thole, J.T., 2008, Geochemical characterization of bentonite beds in the Two Medicine Formation (Campanian, Montana), including a new $^{40}Ar/^{39}Ar$ age: Cretaceous Research, v. 29, p. 373–385.

Fricke, H.C., Foreman, B.Z., and Sewall, J.O., 2010, Integrated climate model-oxygen isotope evidence for a North American monsoon during the Late Cretaceous: Earth and Planetary Science Letters, v. 289, p. 11–21.

Fricke, H. C., Rogers, R.R., Backlund, R., Dwyer, C.N., and Echt, S., 2008, Preservation of primary stable isotope signals in dinosaur remains, and environmental gradients of the Late Cretaceous of Montana and Alberta: Palaeogeography, Palaeoclimatology, Palaeoecology, v. 266, p. 13–27.

Fricke, H. C., Rogers, R.R., and Gates, T., 2009, Hadrosaurid migration: inferences based on stable isotope comparisons among Late Cretaceous dinosaur localities: Paleobiology, v. 35, p. 270–288.

Friedman, I., and O'Neil, J.R., 1977, Compilation of stable isotope fractionation factors of geochemical interest, *in* Fleischer, M., ed., Data of Geochemistry: U.S. Geological Survey Professional Paper: v. 440-KK, p. 1–12.

Garzione, C.N., Molnar, P., Libarkin, J.C., and MacFadden, B.J., 2006, Rapid late Miocene rise of the Bolivian Altiplano: Evidence for removal of mantle lithosphere: Earth and Planetary Science Letters, v. 241, p. 543–556.

Garzione, C.N., Quade, J., Decelles, P.G., and English, N.B., 2000, Predicting paleoelevation of Tibet and the Himalaya from $\delta^{18}O$ vs. altitude gradients in meteoric water across the Nepal Himalaya: Earth and Planetary Science Letters, v. 183, p. 215–229.

Gat, J.R., 1996, Oxygen and hydrogen isotopes in the hydrologic cycle: Annual Review of Earth and Planetary Sciences, v. 24, p. 225–262.

Gill, J.T., and Cobban, W.A., 1973, Stratigraphy and geologic history of the Montana Group and equivalent rocks, Montana, Wyoming, and North and South Dakota: U.S. Geological Survey Professional Paper, v. 776, p. 1–37.

Hasegawa, T., Pratt, L.M., Maeda, H., Shigeta, Y., Okamoto, T., Kase, T., and Uemura, K., 2003, Upper Cretaceous stable carbon isotope stratigraphy of terrestrial organic matter from Sakhalin, Russian Far East: A proxy for the isotopic composition of paleoatmospheric CO_2: Palaeogeography, Palaeoclimatology, Palaeoecology, v. 189, p. 97–115.

Horner, J.R., and Makela, R., 1979, Nest of juveniles provides evidence of family structure among dinosaurs: Nature, v. 282, p. 296–298.

Horton, T.W., and Chamberlain, C.P., 2006, Stable isotope evidence for Neogene surface downdrop in the central Basin and Range Province: Geological Society of America Bulletin, v. 118, p. 475–490.

Hutton, J., 1989, Movements, home ranges, dispersal and the separation of size classes in Nile crocodiles: American Zoologist, v. 29, p. 1033–1049.

Jerzykiewicz, T., and Sweet, A.R., 1987, Semi-arid floodplain as a paleoenvironmental setting of the Upper Cretaceous dinosaurs: Sedimentological evidence from Mongolia and Alberta, *in* Currie, P.J., and Koster, E.H., eds., Fourth Symposium on Mesozoic Terrestrial Ecosystems: Occasional Paper of the Tyrrell Museum of Palaeontology, v. 3, p. 125–128.

Jerzykiewicz, T., and Sweet, A.R., 1988, Sedimentological and palynological evidence of regional climatic changes in the Campanian to Paleocene sediments of the Rocky Mountain Foothills, Canada: Sedimentary Geology, v. 59, p. 29–76.

Kauffman, E.G., 1977, Geological and biological overview: The Western Interior Cretaceous basin: The Mountain Geologist, v. 14, p. 75–99.

Kelly, J.F., 2000, Stable isotopes of carbon and nitrogen in the study of avian and mammalian trophic ecology: Canadian Journal of Zoology, v. 78, p. 1–27.

Kent-Corson, M.L., Sherman, L.S., Mulch, A., and Chamberlain, C.P., 2006, Cenozoic topographic and climatic response to changing tectonic boundary conditions in Western North America: Earth and Planetary Science Letters, v. 252, p. 453–466.

Koch, P.L., 1998, Isotopic reconstruction of past continental environments: Annual Review of Earth and Planetary Science, v. 26, p. 573–613.

Koch, P.L., Hoppe, K.A., and Webb, S.D., 1998, The isotopic ecology of late Pleistocene mammals in North America: Part 1. Florida: Chemical Geology, v. 26, p. 119–138.

Koch, P.L., Tuross, N., and Fogel, M.L., 1997, The effects of sample treatment and diagenesis on the isotopic integrity of carbonate in biogenic hydroxylapatite: Journal of Archaeological Science, v. 24, p. 417–429.

Kohn, M.J., and Cerling, T.E., 2002, Stable isotope compositions of biological apatite: Reviews in Mineralogy and Geochemistry, v. 48, p. 455–488.

Kohn, M.J., and Dettman, D.L., 2007, Paleoaltimetry from stable isotope compositions of fossils: Reviews in Mineralogy and Geochemistry, v. 66, p. 119–154.

Kohn, M.J., Miselis, J.L., and Fremd, T.J., 2002, Oxygen isotope evidence for progressive uplift of the Cascade Range, Oregon: Earth and Planetary Science Letters, v. 204, p. 151–165.

Kolodny, Y., Luz, B., and Navon, O., 1983, Oxygen isotope variations in phosphate of biogenic apatites, I. Fish bone apatite: Rechecking the rules of the game: Earth and Planetary Science Letters, v. 64, p. 398–404.

Leopold, L.B., and Maddock, T., Jr., 1953, The hydraulic geometry of stream channels and some physiographic implications: U.S. Geological Survey Professional Paper, v. 252, p. 1–53.

Morgan, M.E., Behrensmeyer, A.K., Badgley, C., Barry, J.C., Nelson, S., and Pilbeam, D., 2009, Lateral trends in carbon isotope ratios reveal a Miocene vegetation gradient in the Siwaliks of Pakistan: Geology, v. 37, p. 103–106.

Mulch, A., and Chamberlain, C.P., 2007, Stable isotope paleoaltimetry in orogenic belts: The silicate record in surface and crustal geological archives: Reviews in Mineralogy and Geochemistry, v. 66, p. 89–118.

Mulch, A., Graham, S.A., and Chamberlain, C.P., 2006, Hydrogen isotopes in Eocene river gravels and paleoelevation of the Sierra Nevada: Science, v. 313, p. 87–89.

Mulder, T., and Syvitski, J.P.M., 1996, Climatic and morphologic relationships of rivers: Implications of sea-level fluctuations on river loads: The Journal of Geology, v. 104, p. 509–523.

Nelson, B.K., Deniro, M.J., Schoeninger, M., Depaolo, D.J., and Hare, P.E., 1986, Effects of diagenesis on strontium, carbon, nitrogen and oxygen concentration and isotopic composition of bone: Geochimica et Cosmochimica Acta, v. 50, p. 1941–1949.

Patterson, W., Smith, G., and Lohmann, K.C., 1993, Empirical determination of oxygen isotope thermometry in fish aragonitic otoliths, *in* Swart, P., Lohmann, K.C, McKenzie, J., and Savin, S., eds., Climate Changes in Continental Isotopic Records: American Geophysical Union, Monograph, v. 78, p. 191–202.

Poulsen, C.J., Pollard, D., and White, T.S., 2007, General circulation model simulation of the $\delta^{18}O$ content of continental precipitation in the middle Cretaceous: A model-proxy comparison: Geology, v. 35, p. 199–202.

Price, R.A., and Fermor, P.R., 1985, Structure section of the Canadian foreland thrust and fold belt west of Calgary, Alberta: Geological Survey of Canada, Paper, v. 84–14, 1 sheet.

Quade, J., Garzione, C., and Eiler, J., 2007, Paleoelevation reconstruction using pedogenic carbonates: Reviews in Mineralogy and Geochemistry, v. 66, p. 53–87.

Roe, G.H., 2005, Orographic precipitation: Annual Review of Earth and Planetary Sciences, v. 33, p. 645–671.

Rogers, R.R., 1990, Taphonomy of three dinosaur bone beds in the Upper Cretaceous Two Medicine Formation of northwestern Montana: Evidence for drought-related mortality: PALAIOS, v. 5, p. 394–413.

Rogers, R.R., 1994, Nature and origin of through-going discontinuities in nonmarine foreland basin strata, Upper Cretaceous, Montana: Implications for sequence analysis: Geology, v. 22, p. 1119–1122.

Rogers, R.R., 1998, Sequence analysis of the Upper Cretaceous Two Medicine and Judith River Formations, Montana: Nonmarine response to the Claggett and Bearpaw Marine Cycles: Journal of Sedimentary Research, v. 68, p. 615–631.

Rogers, R.R., and Brady, M.E., 2010, Origins of microfossil bonebeds: Insights from the Upper Cretaceous Judith River Formation of north-central Montana: Paleobiology, v. 36, p. 80–112.

Rogers, R.R., Fricke, H.C., Addona, V., Canavan, R.R., Dwyer, C.N., Harwood, C.L., Koenig, A.E., Murray, R., Thole, J.T., and Williams, J., 2010, Using laser ablation-inductively couple plasma-mass spectrometry (LA-ICP-MS) to explore geochemical taphonomy of vertebrate fossils in the Upper Cretaceous Two Medicine and Judith River Formations of Montana: PALAIOS, v. 25, p. 183–195.

Rogers, R.R., and Kidwell, S.M., 2000, Associations of vertebrate skeletal concentrations and discontinuity surfaces in terrestrial and shallow marine records: A test in the Cretaceous of Montana: Journal of Geology, v. 108, p. 131–154.

Rogers, R.R., Swisher, C.C., III, and Horner, J.R., 1993, $^{40}Ar/^{39}Ar$ age and correlation of the nonmarine Two Medicine Formation (Upper Cretaceous), northwestern Montana, U.S.A.: Canadian Journal of Earth Science, v. 30, p. 1066–1075.

Rowley, D.B., 2007, Stable isotope-based paleoaltimetry: Theory and validation: Reviews in Mineralogy and Geochemistry, v. 66, p. 23–52.

Rowley, D.B., and Garzione, C.N., 2007, Stable isotope-based paleoaltimetry: Annual Review of Earth and Planetary Science, v. 35, p. 463–508.

Rozanski, K., Araguás-Araguás, L., and Gonfiantini, R., 1993, Isotopic patterns in modern global precipitation, *in* Swart, P.K., Lohmann, K.C., McKenzie, J.A., and Savin, S., eds., Climate Change in Continental Isotopic Records: American Geophysical Union, Washington, D.C., p. 1–36.

Sears, J.W., 2001, Emplacement and denudation history of the Lewis-Eldorado-Hoadley thrust slab in the Northern Montana Cordillera, USA: Implications for steady-state orogenic process: American Journal of Science, v. 301, p. 359–373.

Shackleton, N.J., and Kennett, J.P., 1975, Paleotemperature history of the Cenozoic and the initiation of Antarctic glaciation: Oxygen and carbon isotope analyses in DSDP sites 277, 279, and 281, *in* Kennett, J.P., Houtz, R.E., et al., eds., Initial Reports of the Deep Sea Drilling Project, v. 29, p. 743–755.

Smith, E.N., 1979, Behavioral and physiological thermoregulation of crocodilians: American Zoologist, v. 19, p. 239–247.

Snedden, G.A., Kelso, W.E, and Rutherford, D.A., 1999, Diel and seasonal patterns of spotted gar movement and habitat use in the lower Atchafalaya River Basin, Louisiana: Transactions of the American Fisheries Society, v. 128, p. 144–154.

Stanton Thomas, K.J., and Carlson, S.J., 2004, Microscale $\delta^{18}O$ and $\delta^{13}C$ isotopic analysis of an ontogenetic series of the hadrosaurid dinosaur *Edmontosaurus*: Implications for physiology and ecology: Palaeogeography, Palaeoclimatology, Palaeoecology, v. 206, p. 257–287.

Talbot, M.R., 1990, A review of the paleohydrological interpretation of carbon and oxygen isotopic ratios in primary lacustrine carbonates: Chemical Geology, v. 80, p. 261–279.

West, J.B., Bowen, G.J., Dawson, T.E., and Tu, K.P., 2010, Isoscapes: Understanding Movement, Pattern, and Process on Earth through Isotope Mapping: Springer, New York 487 p.

Wismer, D.A., and Christie, A.E., 1987, Temperature relationships of great lakes fishes: a data compilation: Great Lake Fishery Commission Special Publication, v. 87-3, p. 1–165.

Wolfe, J.K., and Upchurch, G.R., Jr., 1987, North American nonmarine climates and vegetation during the Late Cretaceous: Palaeogeography, Palaeoclimatology, Palaeoecology, v. 61, p. 33–77.

Yang, C., Telmer, K., and Veizer, J., 1996, Chemical dynamics of the "St. Lawrence" riverine system: δD_{H2O}, $\delta^{18}O_{H2O}$, $\delta^{13}C_{DIC}$, $\delta^{34}S_{sulfate}$, and dissolved $^{87}Sr/^{86}Sr$: Geochimica et Cosmochimica Acta, v. 60, p. 851–866.

ACCEPTED JUNE 16, 2011